Potential Utilization of Grounded Bottom Ash for Sustainable Stowing Applications

KAUSHAL KUMAR[1], JARNAIL SINGH[2], UMANK MISHRA[3], SUBHAV SINGH[4,5], PANKAJ KUMAR[6], NISHANT YADAV[7], PRAWAR[8,*], RISHABH ARORA[9]

[1]Department of Mechanical Engineering,
K. R. Mangalam University, Gurugram, Haryana 122103,
INDIA

[2]Department of Mechanical Engineering,
University Centre for Research and Development,
Chandigarh University, Gharuan, Mohali-140413,
INDIA

[3]Department of Civil Engineering, Guru Ghasidas Vishwavidyalaya,
Bilaspur Chhattisgarh,
INDIA

[4]Centre of Research Impact and Outcome,
Chitkara University,
Himachal Predesh-174103,
INDIA

[5]Division of research and Development,
Lovely Professional University,
Punjab 144411,
INDIA

[6]Department of Production and Industrial Engineering,
NIT Jamshedpur,
831014,
INDIA

[7]Department of Civil Engineering,
Bhilai Institute of Technology,
Durg 490001,
INDIA

[8]Department of Applied Sciences,
K. R. Mangalam University,
Gurugram, Haryana 122103,
INDIA

[9]Department of Civil Engineering,
Amity University,
Gurugram, Haryana 122412,
INDIA

**Corresponding Author*

Abstract: - The present investigation focused on examining the physical, rheological, and mineral aspects of ground bottom ash to enhance comprehension of its utility in the stowing application. Analysis revealed a notable presence of silica in the ash sample, with F-type ash containing alumina and iron oxides while predominant crystalline phases were noticed as quartz and mullite. These characterizations suggest its potential application as stowing material in coal mines, contributing to industry sustainability and mitigating environmental hazards. Experimental results on rheological properties and the impact of concentration on varying pipe diameters indicated a correlation: an increase in pipe diameter led to a slower but evident rise in critical velocity. This data proves invaluable in designing pipeline configurations for stowing bottom ash slurries of differing concentrations and pipe sizes.

Key-Words: - Coal Ash; Ground Ash; Mineral Characterization; Rheology; Stowing; Sustainability.

Received: July 22, 2024. Revised: January 24, 2025. Accepted: March 11, 2025. Published: April 10, 2025.

1 Introduction

A significant amount of energy is obtained from coal, accounting for around 55 % of the world's total energy output. The incineration of pulverized coal in thermal power plants accounts for approximately 70 % of India's total energy production, [1], [2], [3]. The grade of Indian coal that is currently accessible is very low. The Fly Ash (FA) level of Indian coal is extremely high, while its calorific value is relatively low, [4], [5]. Ash percentages range from 34 to 39% in Indian coal, although the same ranges from 10 to 15% in imported coal, [6], [7], [8], [9]. The current status of FA generation in thermal power–plants is shown in Figure 1. Indian thermal power plant produced approximately 270.82 million tons of FA in the financial year 2022, [4]. However, only 95.95 % of this quantity is utilized in various industries, as shown in Figure 2; according to the report released in 2022 by the Central Electricity Authority of New Delhi. This production always raises a question about the sustainability of the thermal and other industries utilizing coal as an energy source. To confirm sustainability, FA is utilized in the production of brick, landfill, soil amendment, and construction sectors due to its remarkable mechanical capabilities, [10], [11], [12]. This study rigorously investigates the physical, rheological, and mineral properties of ground bottom ash, with a particular emphasis on advanced statistical analyses and improved mathematical modeling to ensure robust and reproducible results.

On the other hand, the quantity of FA utilized in concrete production is not an exceptionally significant amount, [13], [14], [15]. The conservative ash disposal system utilizes roughly 631 million m^3 of water every year that acquires area in terms of land higher than 25,000 acres, [16], [17], [18]. Bottom ash production in thermal power plants is growing at an alarming rate, leading to disposal issues and concerns about the environment, [2], [5].

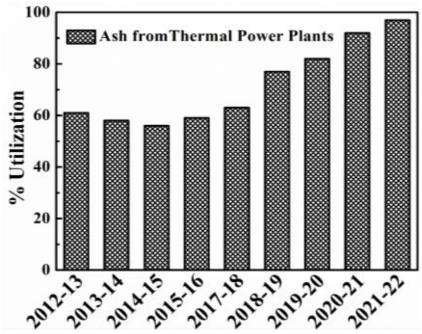

Fig. 1: Current status of utilization of fly ash from thermal power plants in India

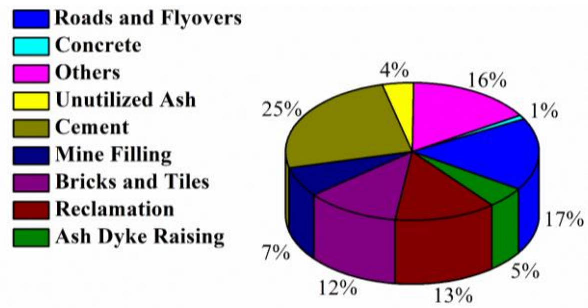

Fig. 2: Utilization of ash in different sectors as per the year 2022

The disposal of ash poses significant risks to the environment, and human and plant health because it contains substantial amounts of hazardous metal elements, [7], [19]. The use of bottom ash in an appropriate manner, the potential risks to the environment can be mitigated, [20], [21]. In addition, the particles that make up bottom ash are more granular than the particles that make up fly ash. Now, bottom ash is used in a variety of applications within civil engineering, including the construction of roads, concrete, structural fill, embankments, and geotechnical applications, [22],

[23]. The characterization tests have been carried out to determine bottom ash's applicability in various applications, all of which have a very low value from a commercial standpoint, [24], [25]. The environmental concerns of bottom ash raised by many researchers, focused their attention on developing strategies for the maximum usage of bottom ash to cut down on its disposal and increase its reclamation.

The current study focuses on exploring the possible use of disposed ground bottom ash as stowing material in coal mines. The ash of the thermal power plant's ash pond has been considered for the investigation. The sample of bottom ash has been tested for its chemical, physical, rheological, and mineralogical characteristics. The present work offers a better understanding of how the ground bottom ash can be utilized. In order to make the sample of ground bottom ash, raw bottom ash was first crushed before being put through a filter with a 355 m opening. For the purpose of determining whether or not ground bottom ash is suitable for use in stowing operations in coal mines, numerous properties have been analyzed. In addition, the rheological characteristics have been investigated to check the effect of pipe diameter on critical velocities. All the above-mentioned testing provides the effective end-use utilization of concerning bottom ash.

2 Materials and Methods

2.1 Materials

For the purpose of testing, a sample pf bottom ash has been taken from Rajiv Gandhi thermal power plant. The samples were collected from the power plant's ash ponds. In order to make the ground bottom ash, a sample of bottom ash was first crushed before being put through a filter with a 355 m opening. Dryness or moisture content has been removed before testing after keeping the sample in the oven at standard temperature.

2.1.1 Notations and Abbreviations

$\tau =$ Shear Stress (Pa)
$\tau_y =$ Yield Stress (Bingham) (Pa)
η = Viscosity (Bingham) (Ns/m^2)
φ = Porosity
δ = Particle Density
ρ = Bulk Density
D = Pipe diameter (m)
WHC= Water Holding Capacity
ϕ = Volume fraction of solids
ρ_f = Carrier Fluid Density (Kg/m^3)
ρ_s = Density of solid particles (Kg/m^3)
V_C=Critical velocity of suspended slurry (m/s)
d = Mean diameter (wt.) of solid particle in Meter
WA_{OD}= Oven dry weight of ash
VA_{AD} = Volume of ash air-dry
WTA_{OD}= Weight of total ash oven dry
PVA= Particle volume of ash
TW_{WA}= Total water in wet ash
WTA_{OD}= Over dry weight of total ash
SS= Sample Size
SD= Standard Deviation
SE= Standard Error
CI=Confidence Interval

2.2 Experimental Method

The chemical and physical properties of the ground bottom ash sample were investigated by different processes. A particle size analyzer (Malvern 3601) was utilized in order to ascertain the range of finer to coarser particles of bottom ash, [26]. Calculations of the bulk density and specific gravity of the sample was carried out with the aid of a water pycnometer in accordance with the prerequisites of International Standard 2386 (Part III). The coefficient of permeability was tested with the ASTM D-2434 standard by using a constant head permeameter [15]. Using Keen's box approach, we were able to determine the amount of water that the ash sample could hold, named as water holding capacity. Some basic physical properties have been measured by using the standard equation 1-4, [27].

$$(\rho) = \frac{WA_{OD}}{VA_{AD}} \tag{1}$$

$$(\delta) = \frac{WTA_{OD}}{PVA} \tag{2}$$

$$(\varphi) = \left(1 - \frac{\rho}{\delta}\right) \times 100 \tag{3}$$

$$WHC = \frac{TW_{WA}}{WTA_{OD}} \times 100 \tag{4}$$

The gravitational settling method yields the maximum solid concentration value in slurry suspension through the static settled concentration. A scanning electron microscopy-energy dispersive X-ray spectrometer (JEOL-6510L) was utilized for analysis of ash sample to evaluate their morphology and chemical character. The X-ray diffraction (XRD) technique was utilized to analyse the mineralogical character of the ground bottom ash sample. A Philips X'Pert diffractometer was used to acquire XRD patterns of ash sample (Model: PW 1710). A typical rheometer (Rheolab Q-C,) which operates according to the Searle principle was utilized to analyse the rheological properties of ash suspension in slurry.

Shear stress measurements at a specific rate were used to determine the slurry's rheological parameter. In order to conduct rheological testing, 100 millilitres ash slurry was prepared by gently mixing necessary amount of water in ash. The shear rate was varied during the rheological tests from 50 to 300 s^{-1}, while the temperature was held constant at 26°C. The rheology was investigated for ash concentrations from 10 to 50 % (by weight).

3 Result and Discussion

3.1 Chemical and Physical Characterization

The information regarding the chemical and physical properties of the ground bottom ash sample is shown in Table 1 (Appendix). The particle size was observed reduced form Table 1 (Appendix), it is due to grinding process which results in finer ash particles. Sample contains 13.77% coarser particles than 90 µm while particles with a size less than 53 µm counted more than 69.25% in the sample. The particle diameters d_{10} to d_{90} were measured for sample as 7.79, 12.05, 18.43, 24.83, 33.32, 43.97, 53.38, 72.7, and 103.6. The value for the static settled concentration was found by making a ash-water suspension with an initial 30% (by weight) ash concentration. The ultimate concentration value in static settled ground bottom ash slurries was determined to be 58.50 (by weight) while a specific gravity of 2.26.

On the other hand, the bulk density was determined to be 1.42 g/cm^3 respectively. It was found that the sample had porosities of 27.60, while their capacities to water holding were found to be 32.15 respectively. After the bottom ash has been ground up, the sample's porosity and water-holding capacity will decrease due to a drop in the air void between the particles and a rise in the mean particle size, [24], [27].

3.2 Mineral and Morphological Characterization

Figure 3 displays the scanning electron microscopy (SEM) at a magnification of x3000 for the ground bottom ash sample. The micrograph provides visual evidence indicating several characteristics of ground bottom ash. Firstly, it reveals that the ash particles have a finer texture, and their appearance appears dark grey, which can be attributed to the presence of unburned carbon, [28]. The surfaces of these particles appear smooth and exhibit a spherical shape. Additionally, the micrograph also highlights the presence of cenospheres in the ground bottom ash. This information was gleaned through the study of the micrograph basically contains (hollow spheres).

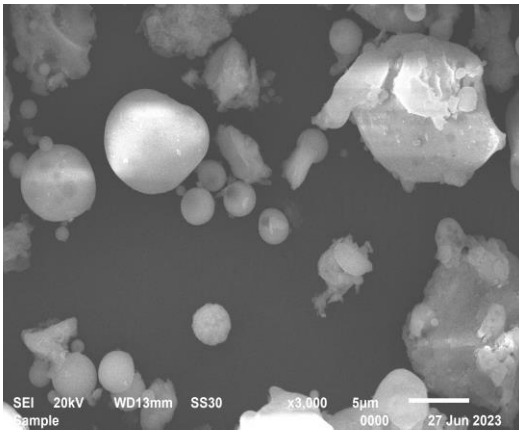

Fig. 3: SEM at a Magnification of x3000 of Sample

Additionally, the observation reveals that certain finer particles, like cenospheres, tend to aggregate with the coarse particles. The existence of cenospheres in ash samples makes it appropriate to use as aggregates in lightweight concrete for sound-absorbing structural applications, [6], [28], [29]. Energy-dispersive X-ray (EDX) spectroscopy was employed to analyze the chemical composition of the ground bottom ash sample. The results of these measurements are presented in Figure 4. It has been noticed that the amount of aluminum oxide and silicon oxide is greater in the sample as a comparison with other elements such as Ti, Fe, K, Mn, Zn, Ca, etc. The presence of SiO_2, Al_2O_3, Fe_2O_4, and CaO in the sample is 51.28%, 36.18%, 4.14%, and 2.84% respectively. The loss of ignition test (LOI) is carried out using ASTM C-311 on the sample to identify the presence of unburned carbon, [30], [31].

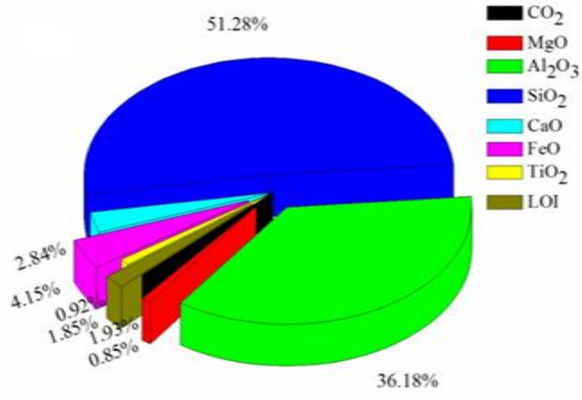

Fig. 4: Chemical composition of the sample

The LOI of the sample was observed as 1.93. The authors have observed that the LOI of coarser coal ash particles has a higher value as compared to finer ash particles, [32], [33], [34]. Figure 5 contains the XRD results of the sample. According to the XRD results, the sample predominantly containscontained quartz and mullite as the major crystalline phases while hematite was also found but least in the least form, [4], [35], [36].

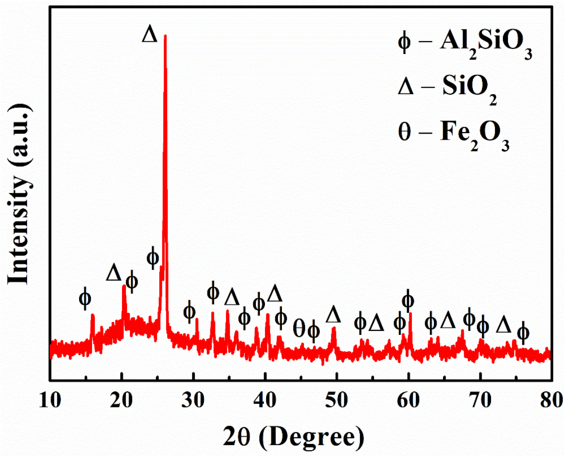

Fig. 5: XRD analysis of ground bottom ash

The values of hematite, mullite, and quartz were noticed as 2.65%, 46.62%, and 50. 72% respectively in the sample. The composition of quartz is mullite is represented by $Al_{(4+2x)}Si_{(2-2x)}O_{(10-x)}$ (x = 0.17 to 0.59), and hematite is composed of Fe_2O_3 and SiO_2. In the ground bottom ash sample, strong peaks corresponding to quartz are observed at approximately 26.639°, while peaks related to mullite are found at approximately 26.214°. Because it contains silica and mullite, it may be used as a building material (like concrete) and as a storage medium, making its application more practical, [37], [38].

3.3 Rheological Analysis

A slurry of ground bottom ash was used as the medium in conducting the rheological test. The solid concentration of 10 to 50 % by weight was considered for analysis. For each sample of ash, the shear stress and rate measurements were obtained. The nature of the slurry was noted as non-Newtonian. The behavior of slurry was modeled as Bingham fluids using the following equation 5:

$$\tau = \tau_y + \eta \frac{du}{dy} \tag{5}$$

τ is the shear stress and η is viscosity while yield stress is τ_y.

The ratio of the slurry's viscosity to water's viscosity when subjected to the same conditions is the definition of relative viscosity. The rigidity coefficient is employed as a substitution for the viscosity of slurry in order to determine the relative viscosity of a Bingham fluid. After fitting a straight-line equation to each and every set of data, we were able to calculate the viscosity of each and every slurry suspension. Figure 6 displays the data on the shear stress and rate at various concentrations. Figure 6 shows that the shear stress increases in a linear fashion alongside an increase in the rate of shear strain. In a suspension of ash slurry with a solid content of 30%, the value of τ_y is always zero (by weight). Based on this information, it can be concluded that slurry samples behave like Newtonian fluids when the solid concentration is at 30% (by weight). However, once this threshold is surpassed, they exhibit non-Newtonian flow properties, [14].

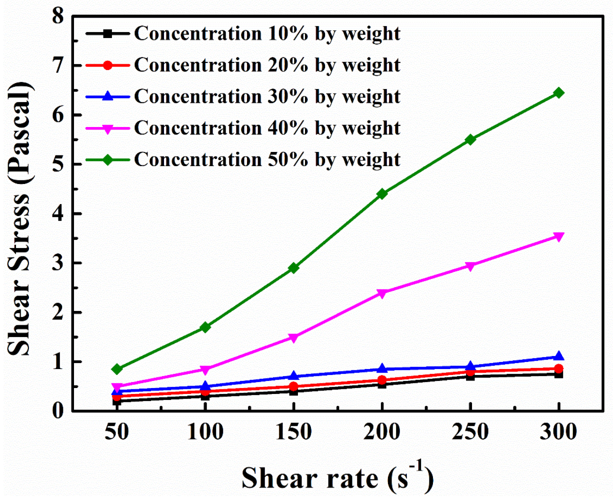

Fig. 6: Shear stress vs. Strain rate relations of sample

It was also observed that the viscosity of slurry is influenced by the quantity of solids present in the mixture. When the solid concentration is lower (up to 30% by weight), the change in relative viscosity is minimal. However, as the concentration of solids increases, the fluctuations in relative viscosity become more significant.

Table 2. Relationship between Slurry Concentration and Standard Deviation with Viscosity

Slurry Conc. (%)	Mean τ	S.D.	Correlation with Viscosity
10	2.5	0.2	0.92
20	4.8	0.3	0.95
30	7.1	0.4	0.96
40	9.5	0.5	0.97
50	12.2	0.6	0.98

The relationship Between Slurry Concentration and Standard Deviation with Viscosity is defined and stated in Table 2.

For each experimental value of shear stress error margin and confidence interval have been measured by using equations 6 and 7.

$$\text{CI} = \text{Mean} \pm (\text{Critical Value} \times \text{SE}) \tag{6}$$

$$SE = \frac{SD}{\sqrt{SS}} \tag{7}$$

Average values have been considered and mean shear stress was found with a margin of error of 0.2 Pa for a 95% confidence level.

In case of higher concentration, the slurry behaves as Bingham fluid and the yield stress value rises proportionally with the increase in concentration. It can also be observed that the shearing process requires a significant amount of shear stress to be initiated when the solid concentration of the slurry is increased.

Numerous researchers who worked with fly ash slurry came to almost similar observations, [39], [40], [41]. The combined amounts of Al_2O_3, SiO_2, and Fe_2O_4 were estimated in the sample as 91.61% of total composition. The LOI is lower than 5%; therefore, the ash conforms to the BS 3892-1(1997) specification as type F. The pozzolanic qualities of the F kind of coal ash are particularly impressive. Coal ash containing fine particles contains a cement-like product that forms when hydrated lime or moisture reacts with alumina and silica, [42], [43]. This reaction takes place in the presence of moisture. Based on experimental research, it was noted that the fine ash of coal can serve as a viable raw material for producing blended cement products. The substantial presence of quartz enhances the mechanical properties of supporting materials, [39], [41].

Additionally, the amount of calcium oxide increases the cementing capabilities of the material, which is then utilized as stow material for mines, [44]. Grounded bottom ash contains more spherical particles, leading to decreased head loss of pipeline as compared to untreated or un-grounded bottom ash. Researchers also drew the same kind of findings with a slurry of mixed fly and bottom ash, [45].

3.4 Calculation of Critical Velocity in Pipe

Calculating the critical velocity for pipelines is the primary application for the correlation as given in equation 8, [46].

$$V_c = 3.116\phi^{\,0.186}\left[2gD\left(\frac{\rho_s-\rho_l}{\rho_l}\right)\right]^{1/2}\left(\frac{d}{D}\right)^{1/6} \tag{8}$$

The amount of solids present in the ground ash slurry suspension might range from 10 to 50% (by weight). For the purpose of calculating the critical velocity in slurry pipelines, the pipe diameter is assumed to be either 50, 100, or 150 mm. When their volume was assessed, it was determined that the ground ash sample had a density of 2240 kg/m^3, respectively. The critical velocity was investigated during the hydraulic stowing operation while the solid content and pipe diameter were varied. Figure 7 illustrates the findings that were discovered during this analysis. It has been noted that the critical velocity increases when both the solid content in the slurry, as well as the pipe diameter, are increased.

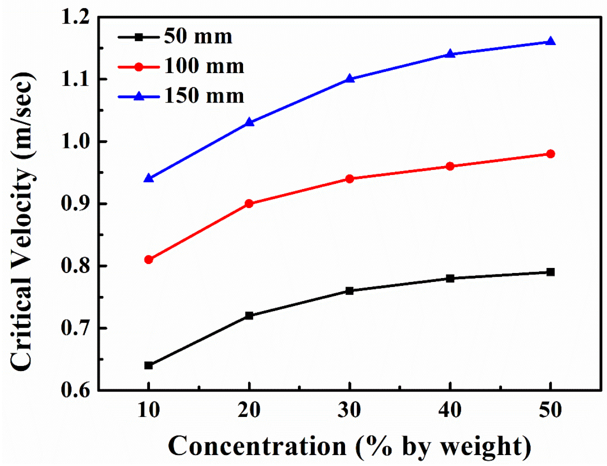

Fig. 7: Relations of Slurry Concentration and Critical Velocity

At 10% concentration, the critical velocity increases from 0.66m/sec to 0.92m/sec by increasing the diameter of the pipe from 50 to 150 mm. This is when the pipe diameter increases from 50 to 200 mm. For other concentrations i.e. 20 to 50% in the sample, the trend was noticed showing an increase in critical velocity and increased from 0.73 to 1.04, 0.77 to 1.08, 0.80 to 1.12, and 0.83 to 1.15 m/sec, respectively. Based on the investigation's results, it was found that the slurry transportation system requires a higher critical velocity when dealing with high concentrations and larger pipe diameters. Only when the ash particles flow at a velocity greater than the critical velocity for a particular pipe diameter and concentration remain suspended in the liquid. This results in the lowest possible pressure drop, [47], [48], [49]. In order to prevent the flow of slurry suspension from becoming blocked or slowed down by the settling of solid particles, the critical velocity must be maintained at or above its value, [50], [51], [52]. The obtained results may be helpful for piping system designers to design a system for stowing ground bottom ash, [53], [54].

3.5 Effect of Varying Pipe Size and Solid Concentration on Critical Velocity

In order to investigate the effect of critical velocity on varying solid concentration, the set of 10% solid concentration has been prepared as 10-20, 20-30, 30-40, and 40-50. The critical velocity of the slurry has been investigated on different pipe sizes e.g. 50mm, 100mm, and 150 mm. Figure 8 represents the effect of variation in the percentage of critical velocity with respect to concentration for different pipe diameters. It has been found that for a 50 mm diameter of the pipe the critical velocity increases 12.3, 6.58, 1.28,3.8 5 with an increase in solid concentration from 10-20, 20-30, 30-40, and 40-50% respectively. While for 100 mm pipe diameter, it is 12.19, 6.52, 2.04, and 4% with an increase in solid concentration from 10-20, 20-30, 30-40, and 40-50% respectively. Similarly, for 150 mm pipe diameter, the critical velocity increased by 10.64, 5.77, 4.55, and 2.61% with an increase in solid concentration from 10-20, 20-30, 30-40, and 40-50% respectively. It has been found that with an increase in pipe diameter the critical velocity increases, but the rate of increment is quite slower as compared to the earlier one.

On the other hand, the effect of solid concentration on critical velocity has been investigated in terms of minimum value to maximum value of critical velocity is shown in Figure 9(a) while the variation for all values of critical velocities for all sets of pipepipe diameter has been investigated and shown in terms of variation per concentration has been shown in Figure 9(b). A solid concentration of 50% has been found as the maximum concentration at which the maximum value of critical velocity has been found. While the least value of critical velocity has been found at 10% of solid concentration.

It was found that the slurry transportation system requires a higher critical velocity when dealing with high concentrations and larger pipe diameters. Only when the ash particles flow at a velocity greater than the critical velocity for a particular pipe diameter and concentration remain suspended in the liquid. This results in the lowest possible pressure drop. In order to prevent the flow of slurry suspension from becoming blocked or slowed down by the settling of solid particles, the critical velocity must be maintained at or above its value. The obtained results may be helpful for piping system designers to design a system for stowing ground bottom ash.

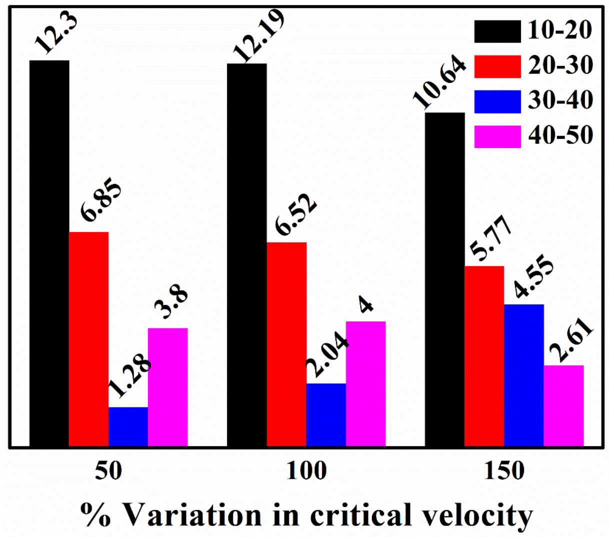

Fig. 8: Variation in percentage of critical velocity with respect to concentration for different pipe diameter

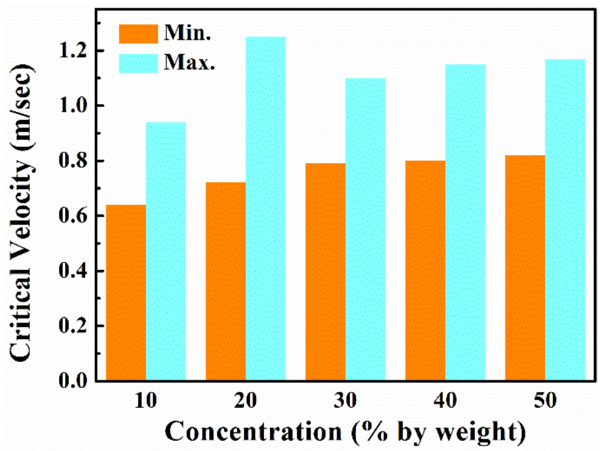

(a)

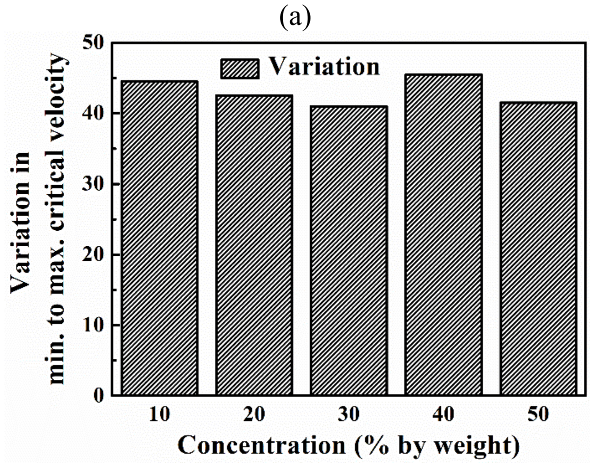

(b)

Fig. 9: (a) Minimum to maximum change in critical velocity for different concentrations with respect to (b)Variation in percentage for different concentration

4 Conclusion

The study focuses on characterizing grounded bottom ash for sustainable use in coal mine stowing. Results from extensive characterization and experimentation have been discussed thoroughly in above section, concluding remarks are as follows:

- Physicochemical, mineral, and rheological properties of ground bottom ash are compared to fly ash, showing similar characteristics.
- Ground bottom ash particles have a finer texture with a dark grey appearance, likely due to unburned carbon, and exhibit smooth surfaces with spherical shapes, making them suitable for stowing applications.
- F-type ground bottom ash demonstrates excellent pozzolanic qualities, advantageous for coal mining storage.
- The viscosity of the ash slurry depends on the solid content in the suspension system.
- Critical velocity results are valuable for designing pipelines capable of hydraulically storing bottom ash slurry at various concentrations and through different pipe sizes.

Utilizing ground bottom ash for mineral storage in mines can reduce transportation costs and environmental risks associated with conventional methods.

References:

[1] V. K. Gahlot, V. Seshadri, and R. C. Malhotra, “Effect of density, size distribution, and concentration of solid on the characteristics of centrifugal pumps,” *Journal of Fluids Engineering, Transactions of the ASME*, vol. 114, no. 3, 1992, doi: 10.1115/1.2910042.

[2] M. Ahmaruzzaman, “A review on the utilization of fly ash,” *Progress in Energy and Combustion Science*, Vol. 36, Issue 3, June 2010, pp.327-363. https://doi.org/10.1016/j.pecs.2009.11.003.

[3] S. H. Kim and H. T. Hahn, “Size effect in particulate metal matrix composites: An analytical approach,” *Advanced Composite Materials: The Official Journal of the Japan Society of Composite Materials*, vol. 15, no. 2, 2006, doi: 10.1163/156855106777873888.

[4] M. H. Fulekar, “Disposal Of Fly Ash—An Environmental Problem,” *International Journal of Environmental Studies*, vol. 26, no. 3, 1986, doi: 10.1080/00207238608710257.

[5] R. Manimaran, I. Jayakumar, R. Mohammad Giyahudeen, and L. Narayanan, “Mechanical properties of fly ash composites—A review,” 2018. *Energy Sources, Part A: Recovery, Utilization, and Environmental Effects*, Vol. 40, Issue 8, 2018. https://doi.org/10.1080/15567036.2018.1463319.

[6] D. P. Mishra and S. K. Das, “A study of physico-chemical and mineralogical properties of Talcher coal fly ash for stowing in underground coal mines,” *Mater Charact*, vol. 61, no. 11, 2010, doi: 10.1016/j.matchar.2010.08.008.

[7] R. Q. Guo, P. K. Rohatgi, and D. Nath, “Preparation of aluminium-fly ash particulate composite by powder metallurgy technique,” *J Mater Sci*, vol. 32, no. 15, 1997, doi: 10.1023/A:1018625118090.

[8] S. Chandel, S. N. Singh, and V. Seshadri, “Deposition characteristics of coal ash slurries at higher concentrations,” *Advanced Powder Technology*, vol. 20, no. 4, 2009, doi: 10.1016/j.apt.2009.06.004.

[9] R. Q. Guo, P. K. Rohatgi, and D. Nath, “Compacting characteristics of aluminium-fly ash powder mixtures,” *J Mater Sci*, vol. 31, no. 20, 1996, doi: 10.1007/BF01159325.

[10] J. David Raja Selvam, D. S. Robinson Smart, and I. Dinaharan, “Microstructure and some mechanical properties of fly ash particulate reinforced AA6061 aluminum alloy composites prepared by compocasting,” *Mater Des*, vol. 49, 2013, doi: 10.1016/j.matdes.2013.01.053.

[11] F. Saba, F. Zhang, S. Liu, and T. Liu, “Reinforcement size dependence of mechanical properties and strengthening mechanisms in diamond reinforced titanium metal matrix composites,” *Compos B Eng*, vol. 167, 2019, doi: 10.1016/j.compositesb.2018.12.014.

[12] A. Bahador, J. Umeda, E. Hamzah, F. Yusof, X. Li, and K. Kondoh, “Synergistic strengthening mechanisms of copper matrix composites with TiO2 nanoparticles,” *Materials Science and Engineering: A*, vol. 772, 2020, doi: 10.1016/j.msea.2019.138797.

[13] H. Yang, L. Jiang, M. Balog, P. Krizik, and J. M. Schoenung, “Reinforcement Size Dependence of Load Bearing Capacity in Ultrafine-Grained Metal Matrix Composites,” *Metall Mater Trans A Phys Metall Mater Sci*, vol. 48, no. 9, 2017, doi: 10.1007/s11661-017-4186-7.

[14] J. B. Ferguson *et al.*, "On the superposition of strengthening mechanisms in dispersion strengthened alloys and metal-matrix nanocomposites: Considerations of stress and energy," *Metals and Materials International*, vol. 20, no. 2, 2014, doi: 10.1007/s12540-014-2017-6.

[15] P. Balamurugan and M. Uthayakumar, "Influence of process parameters on Cu-fly ash composite by powder metallurgy technique," *Materials and Manufacturing Processes*, vol. 30, no. 3, 2015, doi: 10.1080/10426914.2014.984220.

[16] H. Siddhi Jailani, A. Rajadurai, B. Mohan, A. Senthil Kumar, and T. Sornakumar, "Development and properties of aluminium silicon alloy fly ash composites," *Powder Metallurgy*, vol. 54, no. 4, 2011, doi: 10.1179/003258909X12502679013936.

[17] S. Thanga Kasi Rajan, A. N. Balaji, P. Narayanasamy, and S. C. Vettivel, "Microstructural, electrical, thermal and tribological studies of copper-fly ash composites through powder metallurgy," *Bulletin of the Polish Academy of Sciences: Technical Sciences*, vol. 66, no. 6, 2018, doi: 10.24425/bpas.2018.125941.

[18] A. Trivedi and V. K. Sud, "Grain characteristics and engineering properties of coal ash," *Granul Matter*, vol. 4, no. 3, 2002, doi: 10.1007/s10035-002-0114-6.

[19] A. K. Kasar, N. Gupta, P. K. Rohatgi, and P. L. Menezes, "A Brief Review of Fly Ash as Reinforcement for Composites with Improved Mechanical and Tribological Properties," 2020. doi: 10.1007/s11837-020-04170-z.

[20] D. Bouvard, "Densification behaviour of mixtures of hard and soft powders under pressure," *Powder Technol*, vol. 111, no. 3, 2000, doi: 10.1016/S0032-5910(99)00293-4.

[21] Y. Z. Zhu, Z. M. Yin, Z. D. Xiang, and Z. Zhe, "Cold densification behaviour of multiple alloy powder containing Fe-Cr and Fe-Mo hard particles," *Powder Metallurgy*, vol. 51, no. 2, 2008, doi: 10.1179/174329008X284840.

[22] S. Kumar, S. K. Mohapatra, and B. K. Gandhi, "Effect of addition of fly ash and drag reducing on the rheological properties of bottom ash," *International Journal of Mechanical and Materials Engineering*, vol. 8, no. 1, 2013.

[23] E. Gikunoo, O. Omotoso, and I. N. A. Oguocha, "Effect of fly ash addition on the magnesium content of casting aluminum alloy A535," *J Mater Sci*, vol. 39, no. 21, 2004, doi: 10.1023/B:JMSC.0000044906.60260.19.

[24] R. K. Singh, N. C. Gupta, and B. K. Guha, "The leaching characteristics of trace elements in coal fly ash and an ash disposal system of hermal power plants," *Energy Sources, Part A: Recovery, Utilization and Environmental Effects*, vol. 34, no. 7, 2012, doi: 10.1080/15567036.2011.621928.

[25] P. Aggarwal, Y. Aggarwal, and S. M. Gupta, "Effect of Bottom Ash as Replacement of Fine aggregates in concrete," *Asian Journal of Civil Engineering (Building and Housing) Vol.*, vol. 8, no. 1, 2007.

[26] K. Hirota *et al.*, "Optimum conditions for efficient phagocytosis of rifampicin-loaded PLGA microspheres by alveolar macrophages," *Journal of Controlled Release*, vol. 119, no. 1, 2007, doi: 10.1016/j.jconrel.2007.01.013.

[27] E. Egemen and C. Yurteri, "Regulatory leaching tests for fly ash: A case study," *Waste Management and Research*, vol. 14, no. 1, 1996, doi: 10.1006/wmre.1996.0005.

[28] ASTM, "Standard Test Method for Permeability of Granular Soils (Constant Head) using Water Picnometer," *ASTM International, West Conshohocken, Pa*, vol. i, no. Reapproved 2006, 2006.

[29] T. Bakoshi, K. Kohno, S. Kawasaki, and N. Yamaji, "Strength and durability of concrete using bottom ash as replacement for fine aggregate," in *American Concrete Institute, ACI Special Publication*, 1998. doi: 10.14359/6037.

[30] Y. Soong *et al.*, "Dry beneficiation of high loss-on-ignition fly ash," *Sep Purif Technol*, vol. 26, no. 2–3, 2002, doi: 10.1016/S1383-5866(01)00162-9.

[31] P. Sultana, S. Das, B. Bagchi, A. Bhattacharya, R. Basu, and P. Nandy, "Effect of size of fly ash particle on enhancement of mullite content and glass formation," *Bulletin of Materials Science*, vol. 34, no. 7, 2011, doi: 10.1007/s12034-011-0374-z.

[32] P. Ramadoss and T. Sundararajan, "Utilization of Lignite-Based Bottom Ash as Partial Replacement of Fine Aggregate in Masonry Mortar," *Arab J Sci Eng*, vol. 39, no. 2, 2014, doi: 10.1007/s13369-013-0703-1.

[33] K. Kumar and R. Arora, "Effect of additive on rheology of fine particles slurry suspension," in *Materials Today: Proceedings*, 2021. doi: 10.1016/j.matpr.2021.08.330.

[34] J. Singh and A. Chauhan, "A review of microstructure, mechanical properties and wear behavior of hybrid aluminium matrix composites fabricated via stir casting route," 2019. doi: 10.1007/s12046-018-1025-5.

[35] T. C. Eisele, S. K. Kawatra, and A. Nofal, "Tensile properties of class C fly-ash as a foundry core binder," *Mineral Processing and Extractive Metallurgy Review*, vol. 25, no. 4, 2004, doi: 10.1080/08827500390256834.

[36] R. Cheerarot and C. Jaturapitakkul, "A study of disposed fly ash from landfill to replace Portland cement," *Waste Management*, vol. 24, no. 7, 2004, doi: 10.1016/j.wasman.2004.02.003.

[37] T. C. Eisele, S. K. Kawatra, and A. Nofal, "Comparison of class C and class F fly-ashes as foundary sand binders and the effectiveness of accelerators in reducing curing time," *Mineral Processing and Extractive Metallurgy Review*, vol. 25, no. 4, 2004, doi: 10.1080/08827500390256816.

[38] Y. Y. Chun, S. A. S. A. Kadir, A. S. Abdul-Malik, S. N. Syed-Ariftin, S. Z. Mahazer, and Z. Zamzuri, "Characterization of ash derived from combustion of paper mill waste sludge: Comparison with municipal solid waste incinerator ash," *ScienceAsia*, vol. 33, no. 4, 2007, doi: 10.2306/sclenceasia1513-1874.2007.33.473.

[39] T. Matsunaga, J. K. Kim, S. Hardcastle, and P. K. Rohatgi, "Crystallinity and selected properties of fly ash particles," *Materials Science and Engineering: A*, vol. 325, no. 1–2, 2002, doi: 10.1016/S0921-5093(01)01466-6.

[40] M. R. I. Shishir, F. S. Taip, N. A. Aziz, and R. A. Talib, "Physical Properties of Spray-dried Pink Guava (Psidium Guajava) Powder," *Agriculture and Agricultural Science Procedia*, vol. 2, 2014, doi: 10.1016/j.aaspro.2014.11.011.

[41] A. Saker, M. G. Cares-Pacheco, P. Marchal, and V. Falk, "Powders flowability assessment in granular compaction: What about the consistency of Hausner ratio?," *Powder Technol*, vol. 354, 2019, doi: 10.1016/j.powtec.2019.05.032.

[42] C. Igathinathane, L. O. Pordesimo, E. P. Columbus, W. D. Batchelor, and S. R. Methuku, "Shape identification and particles size distribution from basic shape parameters using ImageJ," *Comput Electron Agric*, vol. 63, no. 2, 2008, doi: 10.1016/j.compag.2008.02.007.

[43] P. Verma, R. Saha, and D. Chaira, "Waste steel scrap to nanostructured powder and superior compact through powder metallurgy: Powder generation, processing and characterization," *Powder Technol*, vol. 326, 2018, doi: 10.1016/j.powtec.2017.11.061.

[44] P. K. Gupta, K. Kumar, and A. Kumar, "Study and analysis of domestic ASH & waste glass powder as partial replacement with cement," *International Journal of Civil Engineering and Technology*, vol. 9, no. 11, 2018.

[45] Prawar, Anjali Naithani, H.D. Arora, and Ekata, "Reliability and Cost Assessment of a Plate Manufacturing System with Cold Standby and On-Demand Switching," *Journal of Electrical Systems*, vol. 20, no. 10s, pp. 4864–4873, Jul. 2024, doi: 10.52783/jes.6149.

[46] E. J. Wasp, R. L. Gandhi, and J. P. Kenny, "Solid-liquid flow. Slurry pipeline transportation.," 1975.

[47] F. Inel, M. Khadem, and A. S. Tich Tich, "The Objective Oriented Design of a CUBE Cable - based Parallel Robot for Arm Rehabilitation Tasks," *WSEAS Transactions on Systems*, vol. 23, 2024, doi: 10.37394/23202.2024.23.1.

[48] T. Praharaj, S. P. Swain, M. A. Powell, B. R. Hart, and S. Tripathy, "Delineation of groundwater contamination around an ash pond geochemical and GIS approach," *Environ Int*, vol. 27, no. 8, 2002, doi: 10.1016/S0160-4120(01)00121-0.

[49] D. Das and P. K. Rout, "A Review of Coal Fly Ash Utilization to Save the Environment," 2023. doi: 10.1007/s11270-023-06143-9.

[50] A. K. Saha, "Effect of class F fly ash on the durability properties of concrete," *Sustainable Environment Research*, vol. 28, no. 1, 2018, doi: 10.1016/j.serj.2017.09.001.

[51] A. Bhatt, S. Priyadarshini, A. Acharath Mohanakrishnan, A. Abri, M. Sattler, and S. Techapaphawit, "Physical, chemical, and geotechnical properties of coal fly ash: A global review," *Case Studies in Construction*

Materials, vol. 11, 2019, doi: 10.1016/j.cscm.2019.e00263.

[52] D. K. Nayak, P. P. Abhilash, R. Singh, R. Kumar, and V. Kumar, "Fly ash for sustainable construction: A review of fly ash concrete and its beneficial use case studies," 2022. doi: 10.1016/j.clema.2022.100143.

[53] W. Abbass *et al.*, "Manufacturing of Sustainable Untreated Coal Ash Masonry Units for Structural Applications," *Materials*, vol. 15, no. 11, 2022, doi: 10.3390/ma15114003.

[54] S. Park *et al.*, "Characterization of rare earth elements present in coal ash by sequential extraction," *J Hazard Mater*, vol. 402, 2021, doi: 10.1016/j.jhazmat.2020.123760.

Contribution of Individual Authors to the Creation of a Scientific Article (Ghostwriting Policy)

- Kaushal Kumar carried out the experiments, research and data collection also organized and executed the experiments
- Jarnail Singh, Umank Mishra supervised and carried out experimental calculations also organized and executed the experiments
- Subhav Singh, Pankaj Kumar and Nishant Yadav carried out the simulation, optimization and helped with experiments in the field.
- Rishabh Arora compared and supervised the results of Properties of Ground Bottom Ash.
- Prawar was responsible for the Statistics optimization and software work.

Sources of Funding for Research Presented in a Scientific Article or Scientific Article Itself

No funding was received for conducting this study.

Conflict of Interest

The authors have no conflicts of interest to declare.

APPENDIX

Table 1. Chemical and Physical Properties of Ground Bottom Ash

Particle Size Distribution (µm)		**Particle Size** (µm)	**% Finer**	**pH values for various concentration**		**Other properties**	**Determined Value**
		355	100	**Concentration(%)**	**pH value**	**Porosity(%)**	29.8
		250	98.81				
		150	95.86	10	7.57	**Specific Gravity**	2.24
$\mathbf{d_{10}}$	7.79	**10**	90.72				
$\mathbf{d_{20}}$	12.05	**90**	86.23	20	7.51		
$\mathbf{d_{30}}$	18.43	**75**	81.42			**Capacity of Water Holding(%)**	34.56
$\mathbf{d_{40}}$	24.83	**53**	69.25	30	7.46		
$\mathbf{d_{50}}$	33.32	**26**	42.62				
$\mathbf{d_{60}}$	43.97	**21**	34.18	40	7.41		
$\mathbf{d_{70}}$	53.38	**15**	24.34			**Bulk Density(gm/cm^3)**	1.42
$\mathbf{d_{80}}$	72.7	**11**	19.12	50	7.36		
$\mathbf{d_{90}}$	103.6	**6**	6.15				